Measured lifetimes of selected metastable levels of Ar^{q+} ions ($q=2$, 3, 9, and 10) stored in an electrostatic ion trap

Lisheng Yang,* D. A. Church, Shigu Tu, and Jian Jin†
Physics Department, Texas A&M University, College Station, Texas 77843-4242
(Received 23 August 1993)

Metastable multiply charged argon ions produced in, and extracted from, an electron cyclotron resonance ion source were captured from the beam into an electrostatic (Kingdon) ion trap by rapidly pulsing the potential of the central wire relative to the cylinder. The ions were selected on a charge-to-mass ratio basis before capture. Photons emitted in magnetic-dipole and electric-quadrupole transitions from levels with lifetimes exceeding 5 ms were selected by wavelength and recorded vs ion storage time in the trap. Also, ions were counted after ejection following a preselected storage time in the trap, using a microchannel plate detector. These signals were studied as a function of the pressure of typical residual gases. Extrapolation to zero pressure enabled the extraction of the lifetimes τ of metastable levels from four different configurations of the type ns^2np^k with $n=2$ or 3 and $k=3$, 4, or 5. Our experimental results are $\tau(Ar^{2+},\ 3s^23p^4\,{}^1S_0)=159.7\pm9.7-38.4$ ms, $\tau(Ar^{3+},\ 3s^23p^3\,{}^2P_{3/2})=243\pm73-79$ ms, $\tau(Ar^{9+},\ 2s^22p^5\,{}^2P_{1/2})=8.53\pm0.24-0.17$ ms, and $\tau(Ar^{10+},\ 2s^22p^4\,{}^3P_1)=14.8\pm1.1-0.48$ ms. Both statistical errors and a possible error associated with a systematic correction are given for each measurement. These results are compared with the predictions of theoretical calculations, many previously untested. The basis of the measurement technique is discussed in some detail. The technique is expected to be applicable to ions in a large range of charge states from a variety of low-energy ion sources, and to levels with transitions from the near-infrared to the deep-ultraviolet or soft-x-ray range.

PACS number(s): 32.70.Fw, 32.30.Jc, 95.30.Dr, 52.70.Kz

I. INTRODUCTION

Over the last two decades, there has been a small but continued effort to experimentally determine the lifetimes of long-lived metastable levels of ions using the ion confinement technique [1]. The electrostatic (Kingdon) ion trap [1–3] has been used for a significant fraction of these measurements [4–7]. The motivation for this research is the common observation of "forbidden" magnetic dipole ($M1$), electric quadrupole ($E2$), and intercombination electric-dipole transitions from metastable levels in the tenuous plasmas of astrophysical and laboratory sources, such as the solar corona, gaseous nebulae, and tokamaks [8]. These transitions are prominent, despite their low transition rates, because collision rates are low, and "coronal equilibrium" often prevails [9]. It has been known for many years [10,11] that under such conditions the relative intensities of certain different forbidden, or of allowed and forbidden, transitions can provide important diagnostics of electron density and temperature in the plasmas, provided that the relevant transition probabilities are known. Since experimental information has been sparse and for charge states higher than 2 essentially nonexistent for levels with millisecond lifetimes, numerous theoretical calculations of transition rates of forbidden transitions of increasing sophistication are being carried out. These *ab initio* calculations typically involve the use of approximations and the selection of the configurations to include in the calculation. The accuracy of many of these calculations is difficult to assess and evaluations are usually performed by comparison with other theoretical results, with the implicit assumption that more elaborate efforts are the best. However, recourse to experiment is preferable, and in certain cases for ions with low charge states, factor of 2 differences between experiment and theory, with implications for astrophysical models, have been discovered [12,13]. Semiempirical calculations also require data as input, and even the *ab initio* calculations rely on experimental wavelength determinations.

Several of the metastable lifetime measurements reported here have not previously been reported for ions in high-charge states in any type of ion trap. Ion storage is required since most transitions with lifetimes of microseconds or longer cannot be addressed using ion-beam techniques, due to the spatial extent of the decay length for fast-moving ions. On the other hand, high charge states have not been studied since electron-impact ionization was typically used to produce the metastable ions inside the trap, although recently some success has been achieved in confining charge states to 6+ using colliding plasmas [14]. In the present work, highly charged ions in a beam from a low-energy multicharged ion source were captured into the ion trap. The increasing availability of such ion sources, including the electron cyclotron reso-

*Present address: Advanced Photon Source, Argonne National Laboratory, Argonne, IL 60439-4814.
†Present address: Lawrence Berkeley Laboratory, Bldg. 88, Berkeley, CA 94720.

nance ion source (ECRIS) [15], the electron-beam ion source (EBIS) [16], and the electron-beam ion trap [17,18] when used as a source [19], can be expected to extend this technique to many other charge states and elements. It should be noted that variants of the injection technique can be applied to other types of ion trap and may be superior for certain ions with low charge as well. Once sufficient selected-charge-state current is available, charge-exchange cells or other means can be used to enhance the metastable fraction, although in the measurements reported here, sufficient metastable ions were produced in the ion source.

The basis of the experimental technique is discussed in Sec. II, and the details of individual measurements are featured in Sec. III. An important consideration in the measurements of long lifetimes, particularly for high charge states, is collisional quenching. Although data from the collision measurements are used in the final determination of the experimental lifetimes, the collision measurements and results are of sufficient importance to be discussed in a separate publication [20]. The lifetime measurements are discussed in relation to theoretical calculations in Sec. IV. Several of these measurements have been briefly reported in earlier publications [21,22].

II. EXPERIMENTAL TECHNIQUE

The Kingdon electrostatic ion trap [1–3] conventionally consists of two concentric cylinders terminated axially by two flat plates. When confining positive ions with charge qe and mass m, the central cylinder (usually a wire) is held at a negative potential with respect to the outer cylinder and the terminating caps. Ions with sufficiently low energy but high angular momentum will have stable orbits.

Our Kingdon trap was made from an aluminum cylinder with inner diameter $2a=10$ cm and a concentric tungsten wire with diameter $2b=0.0125$ cm, resulting in a ratio $a/b=800$. The caps were separated by $2c=15$ cm. When a potential $V_0=3.5$ kV was applied to the outer cylinder, and the wire held at $V_w=0$ V, the important parameter $qeV_0/\ln(a/b)\equiv P_0=523.6q$ eV, and the potential energy of a charge qe at radius r near the midplane of the trap was $P(r)=P_0\ln(r/b)=523.6q\ln(r/b)$ eV. In order to confine the ions more closely to the midplane of the trap, the caps were placed at a potential $V_c=3.9$ kV, exceeding V_0. Consequently, the ions were bound by equipotentials of a general cylindrical potential $V(r,z)$, as discussed by Lewis [2]. To the extent that $V(r,z)$ is approximated by a purely radial potential, the virial theorem gives a mean-squared velocity $\bar{v}^2=qe(V_0-V_w)/m\ln(a/b)=P_0/m$, but more generally $\bar{v}^2=(qe/m)\ [\mathbf{r}\cdot\nabla V(r,z)]$. Johnson [3] shows how the potential $V(r,z)$ can be expanded as an infinite sum of modified Bessel functions of zero order, with coefficients determined by the boundary conditions. He notes that, near the trap midplane, orbits are little changed from those of a pure logarithmic potential.

The outer cylinder of the trap was perforated at the midplane by four equally spaced and equally sized apertures about 1.9 cm in diameter. The multicharged ion beam passed into the trap through one aperture, and a significant fraction exited through the opposite aperture to a Faraday cup, when the central wire was held at a potential near that of the cylinder. Just in front of the entrance aperture, a cylinder at zero potential with axis along the ion beam limited the deceleration of the ions upon passing through the cylinder to a small spatial interval near the aperture. This resulted in strong overfocusing, which aided ion capture by providing initial angular momentum relative to the central wire. Capture was also aided by the decreased ion kinetic energy and increased beam density inside the trap as a result of ion retardation [23].

Ions within the trap structure were captured by suddenly reducing the central wire potential V_w to zero in a time $t_w\cong 300$ ns, short compared to the transit time of ions through the trap [24]. The ion beam was then immediately deflected upbeam by applying a potential difference across parallel plates. The ions were held in the trap for a chosen storage interval, up to hundreds of milliseconds, before the wire potential was allowed slowly (about 10 ms) to rise to its original value. During this adiabatic decrease in the confining potential, the mean total ion energy $\bar{E}=[qe(V_0-V_w)/\ln(a/b)][\frac{1}{2}+\ln(r/b)]$ decreased in a way that kept the angular momentum $L=r(mP_0)^{1/2}$ constant, so the orbit radius increased as V_0-V_w was reduced. Some ions which reach the wall of the cylinder pass through the midplane apertures. Behind one aperture a microchannel plate detector was placed. Voltage was applied to this detector after the ion beam was deflected. The emerging ions were accelerated toward the detector by the difference between the external cylinder potential and the detector potential. During the adiabatic increase of the wire potential, pulses were detected over the whole 10-ms interval, short compared to the ion storage time. The total number of pulses detected during this interval provided a measure of the number of ions stored in the trap at the time storage was terminated [23,24].

When short storage times were used, the ion signal was representative of the injected ion number. It was observed that the magnitude of the signal was a strong function of the difference between the incident energy of the beam ions $E_i=qeV_{\rm ext}$ (where $V_{\rm ext}$ was the extraction potential of the ECRIS) and the repulsive potential energy of the trap cylinder $E_0=qeV_0$. The difference $qe|E_i-E_0|$ was approximately the kinetic energy of the ions as they moved inside the Kingdon trap before the central wire potential was decreased. The relation is approximate, because there was some variation of the potentials due to field penetration through the aperture of the cylinder.

Before pulsing the central wire potential, the sum of the ion kinetic and potential energies inside the trap can then be written

$$E_i=qe[V_0+(V_{\rm ext}-V_0)]\ . \tag{1}$$

After V_w is pulsed to zero, the corresponding sum of the energies of the captured ions is

$$E_f=qe(V_{\rm ext}-V_0)+[qeV_0/\ln(a/b)]\ln(r/b)\ , \tag{2}$$

where $E_f < qeV_0$ for stable ion confinement. It is assumed that the potential change is sudden, and that little momentum has been transferred to the ions as a consequence of the rapid potential change. From the relations (1) and (2), $(V_{ext}-V_0) < V_0[1-\ln(r/b)/\ln(a/b)]$ for bound ions, independent of the charge state q. Experimentally, it was found that the potential differences $|V_{ext}-V_0| < 100$ V optimized the stored ion signal. This implies that under optimum conditions, ions occupied the trap out to a radius $r_m \lesssim 0.8a$. When the ion kinetic energy was increased, the ions could be captured only at smaller values of r, reducing the overlap of the ion beam with the volume of stable capture into the trap. For lower than optimum kinetic energies, the increased defocusing of the ion beam by the entrance aperture may have resulted in ion loss at the trap electrodes, depleting the ion number available for confinement. The optimum difference in potentials $|V_{ext}-V_0|$ was determined by small variations in V_0 before lifetime measurements commenced.

An upper limit on the number of ions captured was set by the maximum number within the capture volume when the wire potential was reduced. The number of beam ions in this volume is $N = I\Delta t/qe = (I/qe)2r_m/v$, where I is the ion-beam current and the speed of ions inside the trap

$$v = (2qe|V_{ext}-V_0|/m)^{1/2} = 2.2q^{1/2}\times 10^4 \text{ m/s}$$

for argon ions in these measurements. The result is $N_{max} < 2.3q^{-3/2}\times 10^6$ stored ions per μA of beam current in a single capture. This result ranges between 8×10^5 and 7×10^4 ions per μA, for $2 \le q \le 10$. Currents between 1 and 3 μA were used in all measurements.

The initial distribution of metastable ions within the ground term can be estimated from statistical weights, assuming that all lifetimes are much longer than the beam transport time from the ECRIS to the ion trap $t_t \approx 50$ μs. Table I shows these estimates for the ion charge states studied, based on the details of their ground term level structures. It can be seen that for purposes of estimation, a metastable population of 10% is reasonable, corresponding to between 8×10^4 and 7×10^3 excited ions per μA of beam current, for charge states q between 2 and 10.

During ion detection, ions emerged through an aperture with diameter $D = 1.9$ cm. The relative "detection area" was then $\Delta A/A = \pi D^2/8\pi a L_e \approx 9\times 10^{-3}$, where the effective axial length for trapping, L_e, was estimated to be 10 cm. Assuming that all ions along a radius could possibly be detected during the adiabatic increase in potential, the maximum number of detected ions per cycle is $N_a \lesssim N_{max}\Delta A/A \simeq 2.1q^{-3/2}\times 10^4$. The ion exit times were spread out over about 10 ms, reducing but not eliminating the possible problem of detector dead time in the ion storage measurements. However, far fewer ions were observed in the measurements, perhaps because fewer ions successfully exited the aperture than estimated, due to details associated with individual ion trajectories, and the finite thickness of the aperture wall.

TABLE I. Statistical populations of particular levels of ground terms of multiply charged ions.

Configuration	Statistical population (%)
Ar^{2+} $3s^2 3p^4\ ^1S_0$	6.7
Ar^{3+} $3s^2 3p^3\ ^2P_{3/2}$	20
Ar^{9+} $2s^2 2p^5\ ^2P_{1/2}$	33
Ar^{10+} $2s^2 2p^4\ ^3P_1$	20

Photons from the metastable ion decays were collected using quartz optics, and detected with cooled photomultiplier tubes preselected for a low dark rate. For the Ar^{2+}, Ar^{3+}, and Ar^{9+} measurements, an EMI 9789QB tube was employed, while a red-sensitive EMI 9862QA tube was used for the Ar^{10+} measurement. Interference filters with a 10-nm bandwidth and 10–20 % peak transmission T selected the decay transitions for study. A high-transmission stainless-steel mesh biased about 500 V higher than the trap cylinder voltage was mounted before the first lens to inhibit impingement of fast ions on the surface of the optic.

The fractional solid angle for light collection Ω was no larger than 9×10^{-3}. Using a 20% filter transmission T and an assumed 4% quantum efficiency η for the photomultiplier, along with the mean metastable populations estimated earlier, the number of photons collected during the initial decay time constant $N = N_0\Omega\eta T e^{-1}$ ranged from approximately 2/cycle to 1/cycle per μA of beam current. The dark rate was small and the background negligible in these measurements, and the data were typically accumulated in 10^4 measurement cycles or less, indicating that the estimated photon count rate is in reasonable accord with that actually observed. This leads to the expectation that the estimated ion signal provides a closer approximation to the actual number of ions stored than does the observed ion signal.

The measurement cycle is diagramed in Fig. 1. The decay photon counts were accumulated in a multichannel scalar (MCS) as a function of ion storage time. The ions were then dumped, and the cycle was repeated until the desired signal-to-noise ratio was obtained. The resulting photon decay signals were least-squares fitted to a sum of two exponentials plus a constant background. An initial rapid decrease in intensity was observed for all data, followed by a slower decrease in intensity, which was interpreted as the desired metastable decay. The short-time constant of the initial decrease was associated with stabilization of ions in the trap and the finite time required to deflect the ion beam. Removal of the initial data points enabled a fit to a single exponential plus background, which reproduced the longer time constant of the double exponential fit. An example of this effect appears in Fig. 2, which shows a fitted plot of the logarithm of the data counts vs channel number (time) for Ar^{9+}, without the initial points removed.

The base pressure of the vacuum system during measurements was typically near 3×10^{-9} Torr. It was limited in part by the argon atom flux associated with neutralization of the incident ion beam, and by effusion of gas from the ECRIS beam line, which was operated in the low 10^{-7} Torr range. An analysis with a residual gas analyzer indicated that Ar and N_2 (mass 28 was unlikely

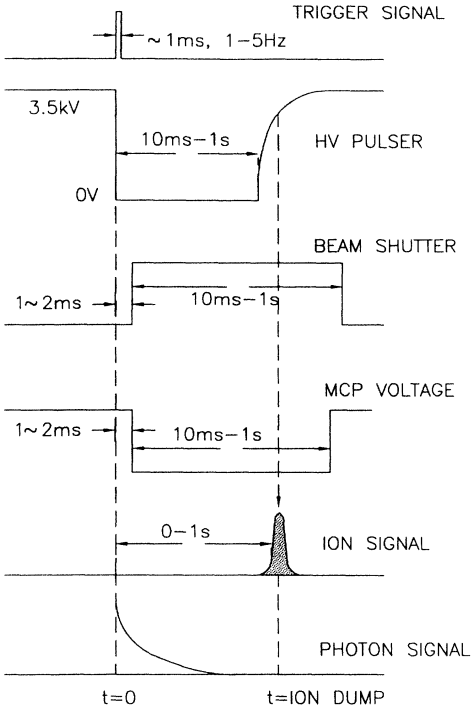

FIG. 1. Measurement cycle used in measurements of lifetimes of metastable levels of ions stored in a Kingdon trap. The ions were captured by rapidly pulsing the potential of the central wire of the trap to zero and were released when the potential rose back to the original value. The ion beam was deflected after the ions were captured and voltage was then applied to the microchannel plate detector. Photons were detected continuously during the ion storage interval. The cycle was repeated many times for signal averaging purposes.

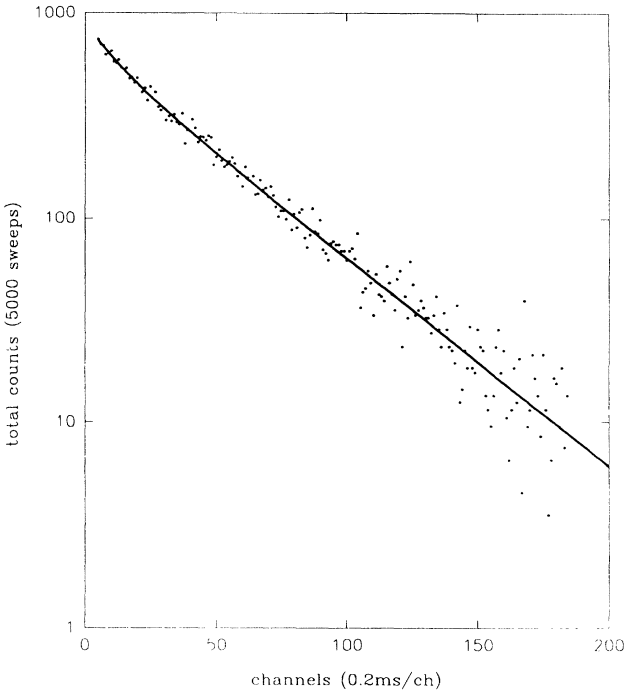

FIG. 2. A plot of the logarithm of the collected photon counts vs channel number (time) for Ar^{9+}, fitted to a sum of two exponentials. A more rapid transient decay during the first few channels can be seen.

to be CO under our measurement conditions) were major constituents, so the metastable lifetimes and ion storage times were studied vs the pressure of these gases, as measured with a nude ion gauge. The gases were separately introduced through a leak valve from an external bakeable gas-handling system. Figure 3 show an example of a plot of reciprocals of measured photon decay time constants vs target gas density. The slope of the graph is a measure of the quenching rate of the metastable level. The rates were extrapolated to zero total pressure to provide an intercept which excluded the effects of residual gas collisions on the metastable lifetime.

When ions change charge in ion-atom collisions at low energies, the initial state of the ion can have a significant effect on the cross section, since little kinetic energy is available to distribute to the products from different initial states. An example is Ar^{2+} in the $3s^2\,3p^4\,{}^1S_0$, ${}^1D_2$, and ${}^3P_{0,1,2}$ levels of the ground term. At thermal energies, the electron capture rate is very low and differs for each state [25]. At eV energies, the capture cross section is increasing rapidly with energy, but level-dependent differences still occur [26]. At the mean ion kinetic energies employed in these lifetime studies, about 500 eV or more, level-dependent differences in electron transfer rates will be smaller; the cross sections are quite large, and depend primarily on the charge state. Nevertheless, a dependence of storage time on metastability cannot be totally disregarded.

The storage time constants of the ions in the trap were measured similarly, in this case by varying the trap "dump" times relative to the time of ion injection. In a collision such as Ar^{9+} (fast)+Ar (slow)$\rightarrow Ar^{8+}$ (fast)+Ar^{+} (slow), if both product ions of the collision were stored in the trap, then the number of observed ions would increase with time, since our detection method provided no charge separation. If only the fast product

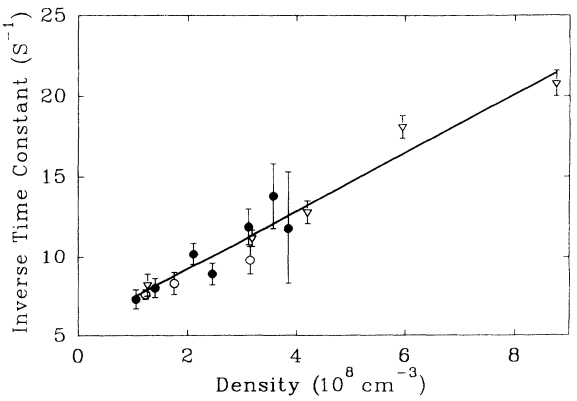

FIG. 3. Reciprocals of the measured photon decay time constants plotted vs density of N_2 target gas for the Ar^{3+} $3p\,{}^2P_{3/2}$ decay. The slope of the plot yields the quenching rate of the metastable level and the intercept provides a measure of the unquenched level lifetime. The lifetime was subsequently corrected for finite time ion storage at zero pressure.

ions were stored, then the ion number would remain constant. We observed a decrease in ion number fitted well by a single exponential plus background, indicating that few if any product ions were stored. This is discussed in more detail in Ref. [20]. The signal-to-noise ratio of the stored-ion data was insufficient to provide improved fits to more complex functional forms. When the reciprocal storage lifetimes from the fits were also plotted vs Ar and N_2 pressure, the reaction rates were similar. The extrapolation to zero total pressure provided a finite intercept, which indicated that the storage time of the ions was limited even in the absence of ion-atom collisions. Results for the limiting storage time for each gas were equal within the error bars. Possibilities include ion-ion collisions or ion loss at the electrodes produced by perturbations of the confining potential. As a test of ion-ion collision effects, measurements were made with similar numbers of Ar^{2+} and Ar^{9+} ions. The collision rates with neutral atoms scaled approximately as the charge, but the intercepts gave comparable limiting storage times. Data with the lowest error limits were obtained using N_2 target gas: $\tau_{is}=427\pm62$ ms for Ar^{9+} and $\tau_{is}=505\pm39$ ms for Ar^{2+}. Consequently, the source of the ion storage limitation in the zero-pressure limit has not been identified as yet.

To obtain the measured metastable level lifetime τ, the time constant τ_u obtained from the extrapolation of the photon decay rate to zero pressure was corrected for the finite storage time limitations τ_{is} according to $1/\tau=1/\tau_u-1/\tau_{is}$. The Ar^{2+} data for τ_{is} were used in the data analysis for Ar^{2+} and Ar^{3+}, and the Ar^{9+} data for Ar^{9+} and Ar^{10+}. The resulting values of τ are tabulated with the errors in τ_u and τ_{is} added in quadrature, and with the value of $\tau-\tau_u$ listed as a possible systematic error.

III. MEASUREMENTS

A. Ar^{2+} $3s^2 3p^4\,{}^1S_0$

The lifetime of this level has been measured twice before in Kingdon traps, on ions produced inside the trap by electron-impact ionization of argon gas. In these earlier measurements [4,7], the ${}^3P_1$-${}^1S_0$ $M1$ branch of the decay near 311 nm was studied, since the decay probability in this branch is about 60%. Alternatively, the ${}^1D_2$-${}^1S_0$ branch near 519 nm can be studied, and in our measurements it is this decay that was emphasized. However, we repeated the earlier measurements and found agreement with results at each wavelength. For example, in a particular comparison of sequential single measurements near base pressure, we obtained an uncorrected lifetime $\tau_u=122.8\pm9$ ms from the 311-nm decay path, and $\tau_u=130.7\pm14$ ms from the 519-nm decay path, in excellent agreement. Both transitions have been observed in the spectra of gaseous nebulae. Level diagrams have been published earlier [4,21].

Because of the relatively long ${}^1S_0$ lifetime, photons were collected out to 400 ms. The beam current ranged between 0.9 and 2.5 μA in individual measurements, and no dependence of the lifetime results on beam current was noted. A total of 30 measurements on the 519-nm transition was carried out with the trap cylinder voltage $V_0=3.5$ kV, and another 37 measurements with $V_0=2.5$ kV, to evaluate the effects of trap potential on the data. Both data sets agreed within the statistical uncertainties, indicating that, e.g., possible second-order Stark mixing was not important. The measured decay constants were extrapolated to zero pressure using argon as a target gas. Less extensive measurements using N_2 as a target gas had larger uncertainties, but did not differ significantly from the data taken using argon. The mean of all measurements, when extrapolated to zero pressure, was $\tau_u=121.3\pm3.4$ ms. This result was then corrected for the effect of finite ion storage time at zero pressure; a correction which is quite small for short decay times, but relatively large for this longer decay time. The final result is $\tau(Ar^{2+},\ 3s^2 3p^4\,{}^1S_0)=159.7\pm9.7,\ -38.4$ ms, where the uncertainties of the separate photon and ion decay times have been added in quadrature, and the shift due to the finite storage time of the ions is listed as a potential systematic error, pending a determination of the origin of the storage time limitation at zero pressure.

Our results can be compared with the data from the earlier Kingdon trap measurements. Prior's [4] uncorrected rate for the Ar^{2+} decay near 311 nm, extrapolated to zero pressure of argon, was $10.7\pm0.8\ s^{-1}$, corresponding to $\tau_u=93.5\pm7$ ms. His zero-pressure ion loss rate was $1.5\pm0.5\ s^{-1}$, so the corrected metastable lifetime was 109^{+36}_{-22} ms. Calamai and Johnson [7] obtain a value of 133 ± 24 ms in their extrapolation to zero argon pressure. They noted that the ion storage time constant was at least twice the time constant for metastable decay, but did not correct their lifetime value for any pressure-independent ion loss. One sees that the earlier measurements are in excellent agreement with our uncorrected measurement, and that the most precise of the two earlier results, that of Calamai and Johnson, agrees adequately with our corrected result as well. This agreement is viewed as satisfactory evidence for the validity of the separate techniques. It should be noted that certain lifetime measurements have been completed in both Kingdon and Paul traps, with excellent agreement [1].

B. Ar^{3+} $3s^2 3p^3\,{}^2P_{3/2}$

The $3p^3\,{}^2P_{1/2}$ and ${}^2P_{3/2}$ levels of Ar^{3+} decay to the ${}^2D_{3/2,5/2}$ levels by $M1$ and $E2$ transitions, and also to the ${}^4S_{3/2}$ level. The predicted lifetime of the ${}^2P_{3/2}$ level is shorter by about a factor of 2. The ${}^4S_{3/2}$-${}^2P_{3/2}$ and ${}^4S_{3/2}$-${}^2P_{1/2}$ transitions have not been observed heretofore, but are calculated to be near 285.4 and 286.8 nm, respectively. The ${}^2D_{3/2}$-${}^2P_{3/2}$ and ${}^2D_{5/2}$-${}^2P_{3/2}$ transitions have been observed [27] with wavelengths of 717.062(100) and 723.726(300) nm, respectively, in excellent agreement with calculations. The transition rates for the ${}^2D$-${}^2P$ branches are lower than those of the ultraviolet ${}^4S$-${}^2P$ branches, however. There is additionally an $M1$ decay between the ${}^2P_{3/2}$ and ${}^2P_{1/2}$ levels, but the decay rate is calculated to be $<10^{-4}\ s^{-1}$. A level diagram appears in Fig. 4.

Since the uv transitions had not previously been ob-

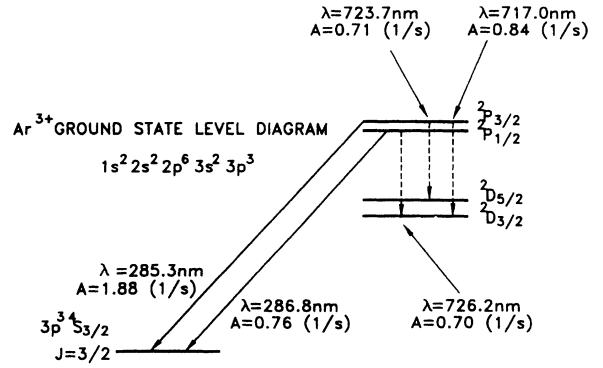

FIG. 4. Level diagram for the decay of the Ar^{3+} $3s^2 3p^3\,^2P_{3/2}$ level.

served, the spectrum near the expected $^4S_{3/2}$-$^2P_{3/2,1/2}$ transition wavelengths was examined with an 0.25-m adjustable-resolution monochromator. Only low-resolution measurements were feasible on these weak lines, and structure in the peak was just visible at a resolution which permitted about 350 counts at the peak in a slow scan. This signal, together with fitted Voigt profiles, appears in Fig. 5. The expected linewidth was 4 nm. The fitted peak ratio of 2.05±0.82 is near the expected value of 2, despite the relatively large error estimate. The fitted wavelengths were 287.8±0.8 and 285.4±0.4 nm. Their separation of 2.4±1.2 nm is, within experimental uncertainty, equal to the separation of the calculated wavelengths of the transition, 1.4 nm. The weighted mean of the fitted wavelengths is 286.2 nm, while the mean of the calculated wavelengths is 286.1 nm. It is highly likely that these are the previously unobserved $^4S_{3/2}$-$^2P_{3/2,1/2}$ transitions of Ar^{3+}, although the observations do not provide a useful check on the calculated wavelengths.

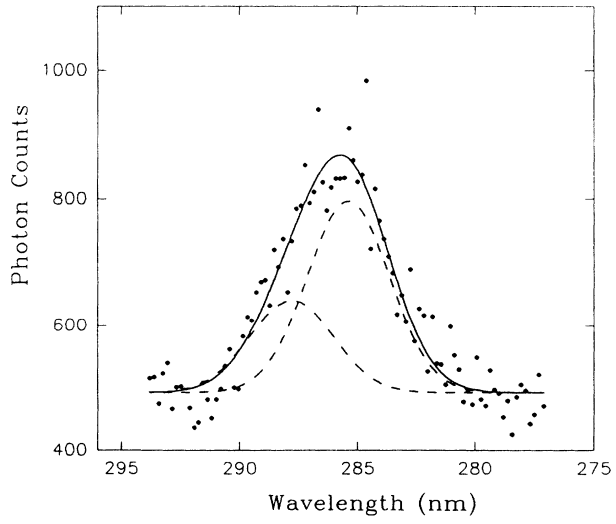

FIG. 5. Observed transition intensity vs wavelength for the $3s^2 3p^3\,^4S_{3/2}$–$^2P_{3/2,1/2}$ transitions of Ar^{3+}. The data were fitted to two Voigt profiles. Resolution was limited to accommodate the low signal intensity of the metastable transitions.

The lifetime measurements were completed using a 10-nm bandwidth interference filter with peak transmission near 280.8 nm, which could not resolve the individual decay components. However, using the calculated wavelengths, the transmission of the filter was twice as high at the wavelength of the transition originating from $^3P_{3/2}$ than that for the $^2P_{1/2}$ transition. Following the filter, the statistical weights then lead to an expected intensity ratio of 4:1. A fit to a sum of two exponentials did not indicate the presence of two long-lived decay components, even when the usual rapid intensity decrease in the initial few channels was removed. Consequently, the single slow decay component was interpreted as the decay of the $^2P_{3/2}$ level, with the much slower, weaker decay of the $^2P_{1/2}$ level appearing as part of the background. Measurements were carried out with ion-beam currents in the 1–3-μA range. Five thousand measurement sweeps per data point were taken. The mean of the zero-pressure intercepts of the Stern-Volmer plots for Ar and N_2 was 6.1±0.86 s^{-1}, leading to an uncorrected time constant $\tau_u = 164 \pm 26$ ms. This constant was corrected for the effect of finite storage time at zero pressure, leading to the final result $\tau(Ar^{3+},\ 3s^2 3p^3\,^2P_{3/2}) = 243 \pm 73\text{-}79$ ms. Again, the correction is large, because the measured lifetime was long. No other measurements of this lifetime exist.

C. Ar^{9+} $2s^2 2p^5\,^2P_{1/2}$

The predominantly $M1$ transition from the $2p^5\,^2P_{1/2}$ to the $2p^5\,^2P_{3/2}$ level occurs near 553 nm. A fit to a sum of two exponentials plus background was again used to account for the rapid initial intensity decrease associated with ion stabilization. A Stern-Volmer plot for argon was constructed from three independent data sets of a total of 26 separate decay measurements collected with $V_0 = 3.5$ kV and beam currents ranging from 2.2 to 3 μA. The result of the extrapolation was $(\tau_u)^{-1} = 118 \pm 3.4\ s^{-1}$. Similar measurements using argon gas and $V_0 = 2.5$ kV resulted in $(\tau_u)^{-1} = 116.7 \pm 2.4\ s^{-1}$. Lower precision data were also accumulated with N_2 gas and with $V_0 = 2.5$ and 3.5 kV. The weighted mean of all of the measurements was $\tau_u = 8.36 \pm 0.12$ ms. The corrected final lifetime is $\tau(Ar^{9+}\ 2s^2 2p^5\,^2P_{1/2}) = 8.53 \pm 0.24\text{-}0.17$ ms, where the correction is now quite small due to the large difference between the metastable lifetime and the limitation on the time of ion storage.

D. Ar^{10+} $2s^2 2p^4\,^3P_1$

The level structure of the ground term of Ar^{10+} can be found in Ref. [21]; it is similar to that of Ar^{2+}, but only the $^3P_2$-$^3P_1$ transition near 693 nm had a convenient wavelength and decay rate for measurements. The calculated lifetime of the $^3P_1$ level is near 15 ms, but the level is fed by transitions from the higher-lying $^1S_0$, $^1D_2$, and $^3P_0$ levels. The $^1S_0$ and $^1D_2$ decays have calculated lifetimes near 0.35 and 3.5 ms, respectively, so these decays will rapidly increase the initial population of $^3P_1$, but will not influence the subsequent decay. The weak $^3P_1$-$^3P_0$ infrared transition has an estimated lifetime ≈330 ms, too

long to affect the measurement in any significant way. This analysis can be quantified by a rate equation for the populations N_i (i=0, 1, and 2) of the $^3P_0$, $^3P_1$, and $^1D_2$ levels:

$$dN_1/dt = -A_1N_1(t) + A_0N_0(0)e^{-A_0t} + \varepsilon A_2N_2(0)e^{-A_2t}, \quad (3)$$

where $A_i = A_i(0) + n\sigma_i\bar{v}$ includes the spontaneous transition rate $A_i(0)$ and the effects of collisional quenching with cross section σ_i. The branching ratio of the $^3P_1$-$^1D_2$ transition is ε=0.15. The $^1S_0$ decay is disregarded because it is so fast compared to the other decays.

Using the predicted value [27] of $A_i(0)$ and an initial statistical distribution among all of the ground-state levels, the solution to Eq. (3) can be written as

$$N_1(t) = 1.23N_1(0)(e^{-A_1t} + 0.01e^{-A_0t} - 0.195e^{-A_2t}) . \quad (4)$$

It is apparent that this equation quantitatively supports the qualitative discussion presented earlier. Since A_2 is relatively large, this term rapidly decreases, while the term with the low value A_0 has a very small relative amplitude. If the first recorded channels of the measured decay are disregarded, the longer time constant can be associated with the $^3P_1$ level decay.

In order to obtain sufficient Ar^{10+} beam current, O_2 was mixed with argon in the ECRIS discharge chamber. Since Ar^{10+} and O^{4+} have the same mass-to-charge ratio, the current through the trap and the confined ion sample contained an unknown fraction of O^{4+} ions. Fortunately, no interfering O^{4+} metastable decays are known. However, due to the mixed charge population, the limiting storage time at zero pressure obtained for Ar^{9+} was used in the data analysis.

Twenty-four decay curves taken as a function of argon pressure at V_0=3.5 kV were extrapolated to zero, yielding τ_u=14.32±0.94 ms. The corrected lifetime is τ(Ar^{10+} $2s^22p^4\,^3P_1$)=14.8±1.1-0.48 ms.

IV. DISCUSSION

The Ar^{2+} $3s^23p^4\,^1S_0$ decay rate has been calculated many times, using different theoretical approximations. Disregarding the earliest calculations (see Ref. [28]), transition probabilities using radial wave functions obtained by the self-consistent field Hartree-Fock method with exchange were obtained by Czyzak and Krueger [28]. Only one configuration was used, but inclusion of exchange, and the calculation of wave functions for each term, provided significant improvements over earlier work. Mendoza and Zeippen [29] used configuration-interaction (CI) optimized wave functions, semiempirical term energy corrections, and relativistic corrections to the Hamiltonian and to the $M1$ operator. Biémont and Hansen [30] used the Hartree-Fock method, including relativistic corrections to the wave functions, and computed energies and spectra in intermediate coupling. Effects of configurations containing $4f$ electrons were included. The most recent calculations are by Saloman and Kim [31], who used a multiconfiguration Dirac-Fock (MCDF) technique, including perturbatively the Breit interaction and the Lamb shift, and experimental and semiempirical fits to energy levels. Results of all of these calculations pertinent to our measurement appear in Table II. The calculations by Mendoza and Zeippen differed from those of Czyzak and Krueger primarily in the determination of the $^1D_2$-$^1S_0$ $E2$ transition rate. Biémont and Hansen agree very well with Mendoza and Zeippen, with the relative differences for the dominant rates less than about 5%. The Saloman and Kim calculations have a higher $M1$ rate, and lower $E2$ rates, resulting in a slightly lower lifetime. Our corrected measurement results favor the calculations of Mendoza and Zeippen, Biémont and Hanson, and Saloman and Kim.

The transition rates from levels of the $3s^23p^3$ configuration of Ar^{3+} have been calculated by several methods. Both $M1$ and $E2$ rates are significant. Biémont and Hansen [32] used Cowan's atomic structure codes for this calculation. Huang [33] used the MCDF code of Desclaux, including all relativistic configurations that correspond to the n=3 shell for odd-parity levels. The Breit interaction and the self-energy and vacuum polarization contributions to the Lamb shift were treated as first-order perturbations. Mendoza and Zeippen [34] note that the effects of configuration interaction were less tractable for an open n=3 shell than for n=2. The first-order spin-orbit interaction vanishes for np^3, causing

TABLE II. Calculated magnetic dipole ($M1$) and electric quadrupole ($E2$) transition rates for the decay of the $3s^23p^4\,^1S_0$ level of Ar^{2+}. Lifetimes determined from the calculated rates are compared with experiment. Numbers in square brackets denote powers of 10.

Ar^{2+} $3s^23p^4$ transition		Transition rates (s^{-1}) CK [28]	MZ [29]	BH [30]	SK [31]
$^3P_2$-$^1S_0$	$M1$				
	$E2$	4.25[−2]	4.17[−2]	3.493[−2]	3.018[−2]
$^3P_1$-$^1S_0$	$M1$	4.02	3.91	3.972	4.166
	$E2$				
$^1D_2$-$^1S_0$	$M1$				
	$E2$	3.10	2.59	2.693	2.575
Net transition rates (s^{-1})		7.1625	6.5417	6.6999	6.7712
Lifetime $^1S_0$ (ms); expt. 159.7±9.7		139.6	152.9	149.3	147.7

TABLE III. Calculated magnetic dipole ($M1$) and electric quadrupole ($E2$) transition rates for the $3s^2 3p^3\ ^2P$ levels of Ar^{3+} and lifetimes determined from the calculated rates. Numbers in square brackets denote powers of 10.

Ar^{3+} $3s^2 3p^3$ transition		Transition rates (s^{-1}) CK [28]	BH [32]	H [33]	MZ [34]
$^4S^{3/2}$-$^2P_{1/2}$	$M1$	0.972	0.954	1.043	0.862
	$E2$	1.19[−4]	3.346[−4]	2.903[−5]	1.84[−5]
$^2D_{3/2}$-$^2P_{1/2}$	$M1$	0.488	0.462	0.464	0.417
	$E2$	0.190	0.193	0.208	0.185
$^2D_{5/2}$-$^2P_{1/2}$	$M1$				
	$E2$	0.122	0.1223	0.1339	0.119
Lifetime ($^2P_{1/2}$) (ms)		564.3	577.5	540.9	631.7
$^4S_{3/2}$-$^2P_{3/2}$	$M1$	2.55	2.336	2.582	2.11
	$E2$	1.56[−5]	9.363[−5]	2.694[−5]	1.09[−6]
$^2D_{3/2}$-$^2P_{3/2}$	$M1$	0.814	0.7635	0.7469	0.693
	$E2$	9.81[−2]	9.643[−2]	0.1063	9.63[−2]
$^2D_{5/2}$-$^2P_{3/2}$	$M1$	0.444	0.4188	0.4251	0.379
	$E2$	0.226	0.2244	0.2449	0.219
Lifetime ($^2P_{3/2}$) (ms)		242	260.5	242.5	285.9
Expt. lifetime 243±73 ms					

transition probabilities to be relatively small. The earlier calculations by Czyzak and Krueger [28] are in rather good agreement with the later calculations. From the calculations tabulated in Table III, the predicted lifetimes range from 541 to 632 ms for the $3P^3\ ^2P_{1/2}$ level, and from 242 to 286 ms for the $3P^3\ ^2P_{3/2}$ level, in each case a range of about 15%. The experimental value of 243 ms supports the faster decay rates, but the large experimental uncertainty encompasses all of the calculations, so no meaningful evaluation can be made.

Early calculations of the transition rates for the Ar^{9+} $2p^5\ ^2 2p^5\ ^2P_{1/2}$ and Ar^{10+} $2p^4\ ^3P_1$ levels were completed by Eidelsberg, Crifo-Magnant, and Zeippen [35]. Cheng, Kim, and Desclaux [36] used the Desclaux MCDF code, including all leading relativistic effects and intrashell correlations. Significant differences in $E2$ rates with the calculations of Zeippen for other configurations were noted, but the $M1$ rates agreed well. Kaufman and Sugar [27] have tabulated rates for many elements and charge states. Table IV shows that the calculated Ar^{9+}

TABLE IV. Calculated total or $M1$ and $E2$ transition rates for the $2s^2 2p^5\ ^2P_{1/2}$ level of Ar^{9+} and the $2s^2 2p^4\ ^3P_1$ level of Ar^{10+} and lifetimes determined from the calculated rates. Numbers in square brackets denote powers of 10.

Ar^{9+} $2s^2 2p^5$ transition		Transition rates (s^{-1}) E, C-MZ [35]	C, KD [36]	KS [28]
$^2P_{3/2}$-$^2P_{1/2}$	$M1$		1.044(2)	
	$M1+E2$	1.05[2]		1.06[2]
	$E2$		2.062[−3]	
Lifetime $^2P_{1/2}$ (ms)		9.52	9.58	9.43
Expt. lifetime 8.53±0.24 ms				
Ar^{10+} $2s^2 2p^4$				
$^3P_2$-$^3P_1$	$M1$		6.556[1]	
	$M1+E2$	67		66.3
	$E2$		4.382[−4]	
Lifetime $^3P_1$ (ms)		14.92	15.25	15.1
Expt. lifetime 14.8±1.1 ms				

lifetimes are about 10% higher than the measured lifetime, but the Ar^{10+} theoretical lifetimes agree well with the measurement.

V. CONCLUSION

A method of injecting ions into a Kingdon trap has been discussed, together with results of measurements of metastable lifetimes of certain levels of Ar^{2+}, Ar^{3+}, Ar^{9+}, and Ar^{10+}. The data for Ar^{2+} agree well with earlier measurements completed using slightly different methods, and all of the data are in adequate agreement with contemporary theoretical calculations. The Ar^{3+} measurement had a relatively low precision (about 25%) but the other lifetime measurements had relative precisions ranging from 3% to 7.5% adequate to test the theoretical calculations, although not sufficient to distinguish the best calculation. Several of these measurements are in charge states $q > 2$, which have not been feasible to study by other methods. This technique opens metastable lifetime measurements to a broad range of charge states, elements, and transitions. It is now potentially feasible to measure lifetimes of all transitions of a configuration by choosing elements and charge states which have transitions with appropriate wavelengths and lifetimes.

ACKNOWLEDGMENTS

This research has been continuously supported by the Robert A. Welch Foundation, and was initiated and completed with support from the National Science Foundation. We thank Professor D. Youngblood and Professor J. Natowitz for permitting the use of the Texas A&M Cyclotron Institute ECRIS for these measurements, during times when it was not needed for cyclotron operations. Professor R. L. Watson and Professor R. E. Tribble, Dr. B. Bandong, and Mr. C. Assad are thanked for their collaboration on the low-energy beam-line design, assembly, and operation. Dr. D. May and Dr. G. Mouchaty provided expert assistance and advice on ECRIS operation. D.A.C. thanks Dr. C. Guet, Dr. J. P. Desclaux, and Dr. S. Blundell for theoretical advice and encouragement of this work.

[1] D. A. Church, Phys. Rep. **228**, 254 (1993).
[2] R. R. Lewis, J. Appl. Phys. **53**, 3975 (1982).
[3] C. E. Johnson, J. Appl. Phys. **55**, 3207 (1984).
[4] M. H. Prior, Phys. Rev. A **30**, 3051 (1984).
[5] A. G. Calamai and C. E. Johnson, Phys. Rev. A **42**, 5425 (1990).
[6] A. G. Calamai and C. E. Johnson, Phys. Rev. A **44**, 218 (1991).
[7] A. G. Calamai and C. E. Johnson, Phys. Rev. A **45**, 7792 (1992).
[8] H. Olthof, *Atoms and Molecules in Astrophysics,* edited by T. R. Carson and M. J. Roberts (Academic, New York, 1972), p. 321.
[9] P. L. Dufton and A. E. Kingston, Adv. At. Mol. Phys. **17**, 355 (1981).
[10] A. H. Gabriel and C. Jordan, Case Stud. At. Phys. **2**, 210 (1972).
[11] G. A. Doschek, in *Autoionization,* edited by A. Temkin (Plenum, New York, 1985), p. 171.
[12] B. C. Johnson, P. L. Smith, and R. D. Knight, Astrophys. J. **281**, 477 (1984).
[13] R. D. Knight, Phys. Rev. Lett. **48**, 792 (1982).
[14] V. H. S. Kwong, Z. Fang, Y. Jiang, T. T. Gibbons, and L. D. Gardner, Phys. Rev. A **46**, 201 (1992).
[15] R. Geller and B. Jacquot, Nucl. Instrum. Methods Phys. Res. **202**, 399 (1982).
[16] E. D. Donets, Phys. Scr. **T3**, 11 (1983).
[17] M. A. Levine, R. E. Marrs, J. R. Henderson, D. A. Knapp, and M. B. Schneider, Phys. Scr. **T22**, 157 (1988).
[18] R. E. Marrs, M. A. Levine, D. A. Knapp, and J. R. Henderson, Phys. Rev. Lett. **60**, 1715 (1988).
[19] D. Schneider, D. DeWitt, M. W. Clark, R. Schuch, C. L. Cocke, R. Schmieder, K. J. Reed, M. H. Chen, R. E. Marrs, M. Levine, and R. Fortner, Phys. Rev. A **42**, 3889 (1990).
[20] D. A. Church, Lisheng Yang, and Shigu Tu (unpublished).
[21] Lisheng Yang and D. A. Church, Phys. Rev. Lett. **70**, 3860 (1993).
[22] Lisheng Yang and D. A. Church, in *The Physics of Highly Charged Ions,* edited by P. Richard, M. Stöckli, C. L. Cocke, and C. D. Lin, AIP Conf. Proc. No. 274 (AIP, New York, 1993), p. 549.
[23] Lisheng Yang, D. A. Church, G. Weinberg, and Qi Wang, Nucl. Instrum. Methods Phys. Res. Sect. B **79**, 37 (1993).
[24] Lisheng Yang and D. A. Church, Nucl. Instrum. Methods Phys. Res. Sect. B **56**, 1185 (1991).
[25] R. Johnson and M. A. Biondi, Phys. Rev. A **20**, 87 (1979).
[26] H. M. Holzscheiter and D. A. Church, J. Chem. Phys. **74**, 2313 (1981).
[27] V. Kaufman and J. Sugar, J. Phys. Chem. Ref. Data **15**, 321 (1986).
[28] S. J. Czyzak and T. R. Krueger, Mon. Not. R. Astron. Soc. **126**, 177 (1963).
[29] C. Mendoza and C. J. Zeippen, Mon. Not. R. Astron. Soc. **202**, 981 (1983).
[30] E. Biémont and J. E. Hansen, Phys. Scr. **34**, 116 (1986).
[31] E. B. Saloman and Y.-K. Kim, At. Data Nucl. Data Tables **41**, 339 (1989).
[32] E. Biémont and J. E. Hansen, Phys. Scr. **31**, 5609 (1985).
[33] K.-N. Huang, At. Data. Nucl. Data Tables **30**, 313 (1984).
[34] C. Mendoza and C. J. Zeippen, Mon. Not. R. Astron. Soc. **198**, 127 (1982).
[35] M. Eidelsberg, F. Crifo-Magnant, and C. J. Zeippen, Astron. Astrophys. **43**, 455 (1981).
[36] K. T. Cheng, Y.-K. Kim, and J. P. Desclaux, At. Data Nucl. Data Tables **24**, 111 (1979).

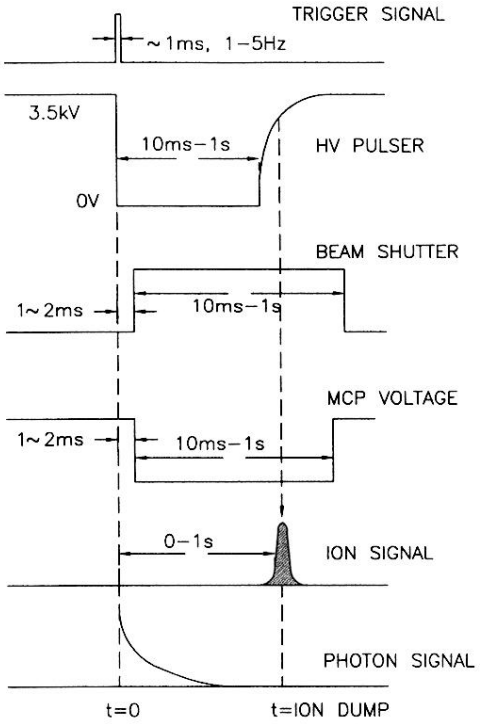

FIG. 1. Measurement cycle used in measurements of lifetimes of metastable levels of ions stored in a Kingdon trap. The ions were captured by rapidly pulsing the potential of the central wire of the trap to zero and were released when the potential rose back to the original value. The ion beam was deflected after the ions were captured and voltage was then applied to the microchannel plate detector. Photons were detected continuously during the ion storage interval. The cycle was repeated many times for signal averaging purposes.